Laser and Particle Beams (2008), *26*, 411–423. Printed in the USA.

doi:10.1017/S0263034608000426

Simulations of a solid graphite target for high intensity fast extracted uranium beams for the Super-FRS

N.A. TAHIR,[1] H. WEICK,[1] A. SHUTOV,[2] V. KIM,[2] A. MATVEICHEV,[2] A. OSTRIK,[2] V. SULTANOV,[2] I.V. LOMONOSOV,[2] A.R. PIRIZ,[3] J.J. LOPEZ CELA,[3] AND D.H.H. HOFFMANN[4]

[1]Gesellschaft für Schwerionenforschung Darmstadt, Darmstadt, Germany
[2]Institute of Problems of Chemical Physics, Chernogolovka, Russia
[3]E.T.S.I. Industriales, Universidad de Castilla-La Mancha, Ciudad Real, Spain
[4]Institut für Kernphysik, Technische Universität Darmstadt, Darmstadt, Germany

(RECEIVED 22 April 2008; ACCEPTED 1 June 2008)

Abstract

Extensive numerical simulations have been carried out to design a viable solid graphite wheel shaped production target for the super conducting fragment separator experiments (Super-FRS) at the future Facility for Antiprotons and Ion Research (FAIR) using an intense uranium beam. In this study, generation, propagation and decay of deviatoric stress waves induced by the beam in the target, have been investigated. Maximum beam intensities that the target can tolerate using different focal spot sizes that are determined by requirements of good isotope resolution and transmission of the secondary beam through the fragment separator, have been calculated. It has been reported elsewhere that the tensile strength of graphite significantly increases with temperature. To take advantage of this effect, calculations have also been done in which the target is preheated to a higher temperature, that in practice can be achieved, for example, by irradiating the target with a defocused ion beam before the experiments are performed. We report results of a few examples using an initial temperature of 2000 K. This study has shown that employing such a configuration, one may use a solid graphite production target even for the maximum intensity of the uranium beam (5×10^{11} ion per bunch) at the Super-FRS.

Keywords: Elastic plastic behavior; Fragment separator; FAIR; High energy density physics; Intense heavy ion beams; Radioactive beams

1. INTRODUCTION

Over the past few years, extensive theoretical work has been carried out to design a production target for the super conducting fragment separator experiments (Super-FRS (Geissel *et al.*, 2003)) at the future Facility for Antiprotons and Ion Research (FAIR (Henning, 2004)) at Darmstadt. Solid graphite (Tahir *et al.*, 2003*b*, 2005*c*, 2007*d*, 2008) as well as liquid jet metal targets (Tahir *et al.*, 2007*e*) have been considered.

According to the design parameters, this new facility will deliver high quality particle beams including uranium with very high intensities. It is expected that in the case of uranium, about 5×10^{11} particles per spill will be delivered, whereas for light and medium heavy elements, the intensities would be even higher. A wide range of particle energies (400 MeV/u–2.7 GeV/u) will be available while the beam is focused to a spot of 1 mm radius. Both, fast and slow extraction options will be available for the beam. In the former case, the bunch length will be on the order of 50–100 ns, while in the latter case, one will have a quasi-uniform beam power. Unlike high energy density (HED) experiments (Tahir *et al.*, 1999, 2000*a*, 2000*b*, 2001*a*, 2001*b*, 2003*a*, 2005*a*, 2005*b*, 2005*d*, 2005*e*, 2006, 2007*a*, 2007*b*, 2007*c*; Piriz *et al.*, 2002, 2003, 2005, 2006, 2007*a*, 2007*b*, Temporal *et al.*, 2003, 2005; Lopez Cela *et al.*, 2006; Hoffmann *et al.*, 2005) in which the target is destroyed in the experiment, the Super-FRS production target should survive over an extended period of time during the experimental campaign carried out at a repletion rate of 1 Hz.

Previous theoretical investigations have shown (Tahir *et al.*, 2003*b*, 2005*c*, 2008) that due to the huge instantaneous power deposition by fast extracted beams (up to 100 GW in case of full intensity of a high-Z beam) at FAIR, a solid Super-FRS production target will always be destroyed in a single experiment, unless one uses a large focal spot to reduce the specific power deposition to an acceptable level.

Address correspondence and reprint requests to: N.A. Tahir, Gesellschaft für Schwerionenforschung Darmstadt, Planckstrasse 1, 64291 Darmstadt, Germany. E-mail: n.tahir@gsi.de

Since the focal spot size is restricted by issues of transmission of the secondary beam through the fragment separator and isotope resolution, it is not possible to increase the focal spot arbitrarily. A delicate balance is required among various parameters in order to satisfy these conflicting requirements simultaneously.

Two important parameters determine whether a solid production target will survive or be destroyed in a single experiment. First, the temperature should remain well below the melting or sublimation temperature of the target material. Second, the deviatoric stresses induced by the beam in the target should be low enough compared to the tensile strength of the material so that the Von Mises criterion is satisfied that means that the Von Mises parameter, M, is always less than 1. In such a case, the material remains in an elastic regime and no permanent damage is inflicted to the target.

Solid graphite is a very attractive material as it has a very high sublimation temperature of 3925 K and has already been tested and used at other facilities for construction of production targets (Heidenreich, 2002) for continuous beams. However, such target concept has never been employed in practice for very high intensity fast extracted beams like the ones at the Super-FRS. Due to the technical challenges involved in construction and operation of a liquid metal jet target, it is highly desirable to develop a solid target for the full intensity of the uranium beam at FAIR. Since Super-FRS experiments will be carried out at a repetition rate of 1 Hz, it is necessary to remove heat from the target efficiently to avoid accumulation of the deposited energy that will eventually lead to target destruction after multiple irradiations. It has been proposed to use a wheel shaped graphite target that is rotated at a suitable frequency so that the same part of the target is not exposed to the beam consecutively, and by the time this part is again irradiated by the projectile particles, it is substantially cooled due to thermal conduction and radiation losses. Detailed numerical simulations of such a scheme have been reported previously (Tahir *et al.*, 2005*c*), which have shown that this concept can be employed successfully in case of a solid graphite Super-FRS target.

In a recent study (Tahir *et al.*, 2008), we investigated the problem of beam induced deviatoric stresses in a solid graphite cylindrical target that is irradiated along the axis. A very important outcome of this study is that circular geometry is much more superior to elliptic shape of the spot as the former generates minimum pressure gradients compared to the latter. As a consequence, the stress level generated in a target irradiated with a perfectly circular focal spot is significantly less than that produced by an elliptic focal spot for the same specific energy. In the present paper, we present two-dimensional (2D) numerical simulations of thermodynamic and hydrodynamic behavior of a solid graphite wheel that is irradiated with a uranium beam. The main purpose of this work is to investigate if it would be possible to design a configuration in which a solid target can be used for the full intensity of the uranium beam. This study has shown that it is possible to use a solid graphite production target with the full intensity of the uranium beam at FAIR, provided certain conditions regarding the beam and the target parameters are fulfilled.

In Section 2, we discuss the problem of beam transmission and isotope resolution while different cases of beam-target configuration used in this study are described in Section 3. Numerical simulations are presented in Section 4, whereas conclusions drawn from this work are noted in Section 5.

2. INFLUENCE OF SPOT SIZE ON ISOTOPE TRANSMISSION AND RESOLUTION

The pulsed fragment beam shall be injected into the collector ring (CR) storage ring after being separated in the Super-FRS. This means the ions must not only be transmitted through the Super-FRS but must also fulfill the criterion for stable motion over millions of turns in the CR. This limits the shape of the accepted transverse phase space to an exact

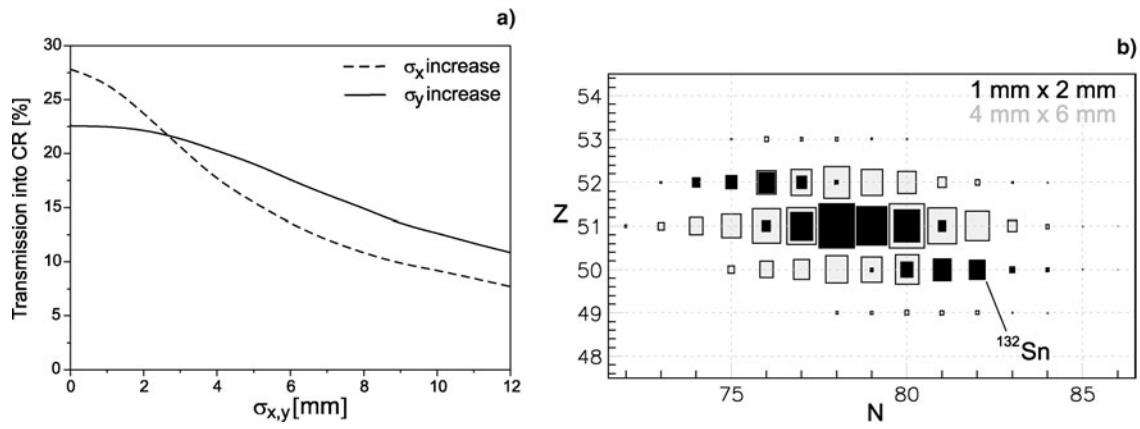

Fig. 1. (**a**) Dependence of the transmission into the CR on the spot size in the *x* and *y*-direction varied independently. While one parameter was changed the other one was kept constant at $\sigma_x = 4$ mm or $\sigma_y = 6$ mm, respectively; (**b**) Nuclides with neutron number (*n*) and proton number (*Z*) remaining after separation in the Super-FRS set for ^{132}Sn, black for a small beam spot of 1 × 2 mm and gray for a larger spot of 4 × 6 mm (sigma). The intensity is proportional to the box size. The total number of ions increased by a factor of 2.2.

https://doi.org/10.1017/S0263034608000426 Published online by Cambridge University Press

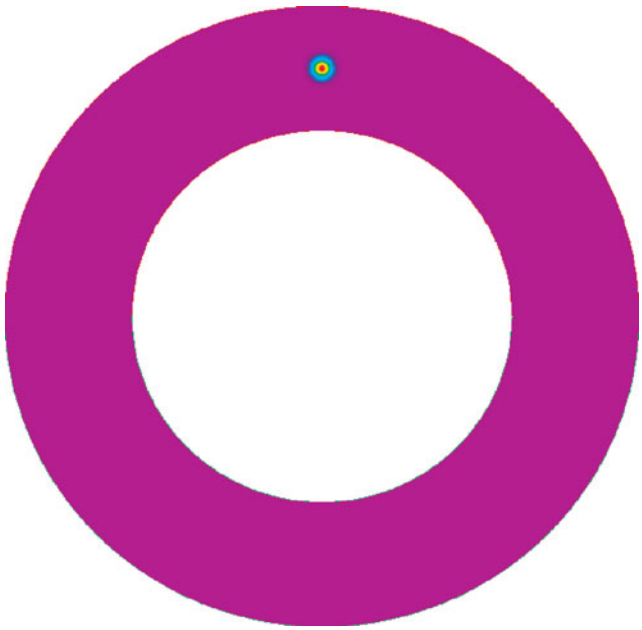

Fig. 2. (Color online) Beam-target geometry.

ellipse with an area of 200 π mm mrad in horizontal (x) and vertical direction (y). It also causes an additional limit on the longitudinal momentum acceptance of $\Delta p/p = \pm 1.75\%$. The numbers can vary depending on the CR setting but these are the present values in the mode foreseen for stochastic cooling of radioactive ion beams (Dolinskii *et al.*, 2004).

From the enlarged phase space area it becomes clear that the transmission must become worse when enlarging the beam spot. However, the initial spot size is not the only contribution to the final emittance of the beam at the exit of the Super-FRS or entrance to the CR. Angular and energy-loss straggling in the degraders used to obtain the separation of different elements due to different energy loss contributes as well and are independent of the initial spot size. In addition, image aberrations also broaden the beam at the exit. The relative importance of these contributions becomes less for a wider beam spot. Therefore, small variations of the spot size does not enter directly proportional in the emittance at the exit of the Super-FRS. Only for larger spots, the emittance becomes proportional to the initial spot size and so do the losses in transmission.

To determine the transmission, the fragment ^{132}Sn produced from fission of ^{238}U was simulated in a Monte-Carlo simulation using the MOCADI code (Iwasa *et al.*, 1997). The primary beam had an energy of 1500 MeV/u and the

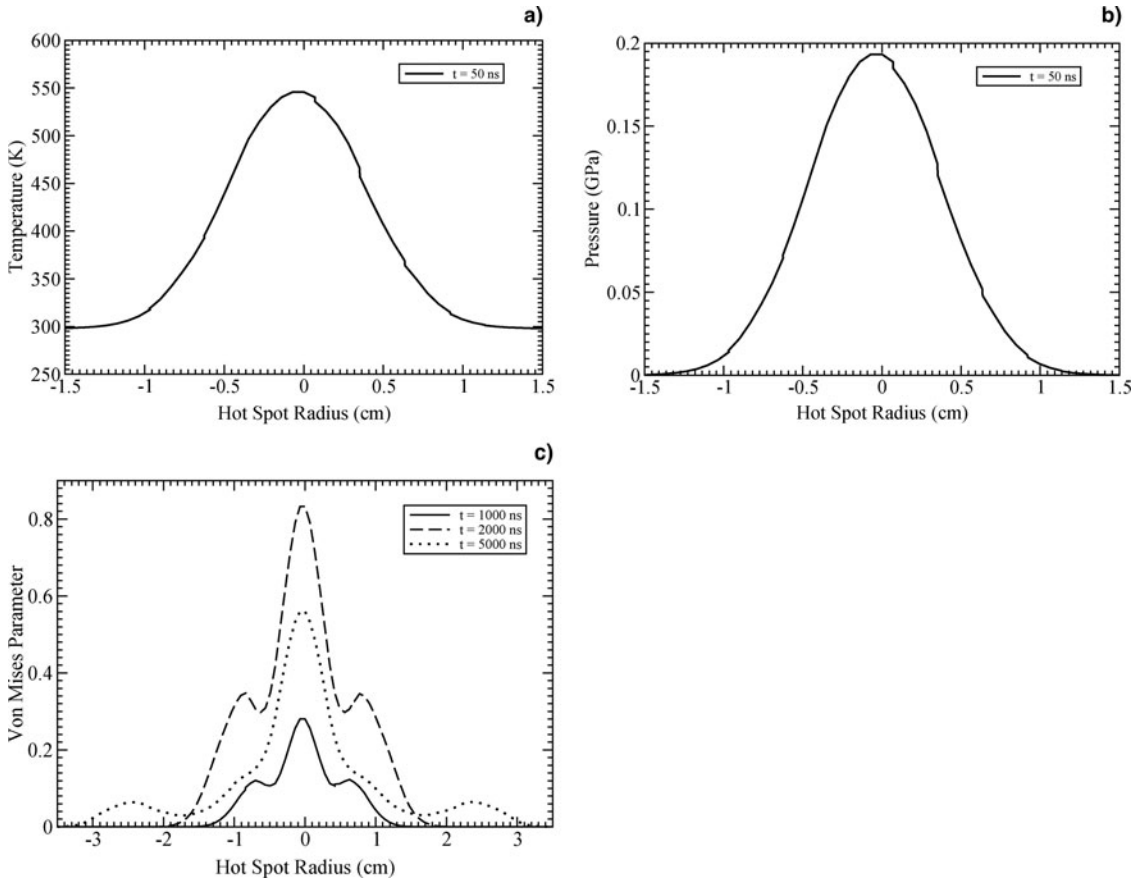

Fig. 3. $N = 10^{11}$ uranium ions per bunch, particle energy = 1 GeV/u, $\tau = 50$ ns, circular focal spot with Gaussian transverse intensity distribution, $\sigma = 4$ mm, initial target temperature = 300 K, yield strength = 70 MPa: (**a**) temperature along spot radius at $t = 50$ ns; (**b**) pressure along spot radius at $t = 50$ ns; (**c**) Von Mises Parameter at three different times (maximum value at $t = 2000$ ns).

https://doi.org/10.1017/S0263034608000426 Published online by Cambridge University Press

fragments were slowed down in the target and the degraders to 740 MeV/u. This provides also enough degrader thickness for reasonable separation. A cut in the size of the CR acceptance was put on the distribution of the ions at the exit of he Super-FRS and the number of ions counted. The result is shown in Figure 1a as a function of the spot size on the target. The transmission into the CR for a small spot of σ_x= 1 mm × σ_y = 2 mm would be 34%. With the spot increased to σ_x = 4 mm and σ_y = 6 mm, still half of this value can be achieved, even though the area was increased by a factor of 12. Compared to a similar older calculation (Tahir *et al.*, 2005*c*) the optics of the Super-FRS was adjusted for the enlarged spot in the *y*-direction. This helps to avoid losses in the Super-FRS.

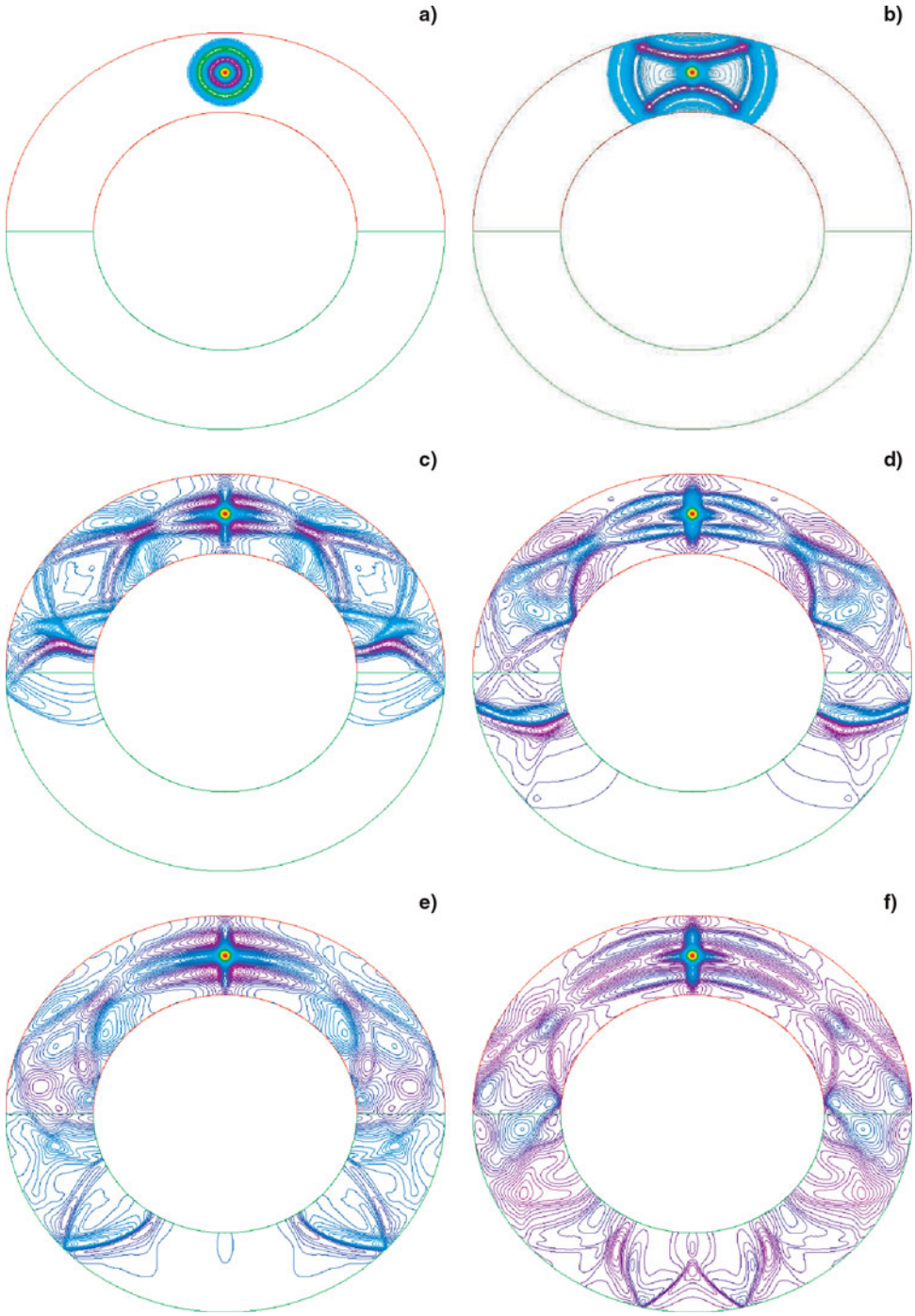

Fig. 4. (Color online) Spreading of pressure waves from the beam heated region; (**a**) t = 5 μs, P_{max} = 55 MPa; (**b**) t = 15 μs, P_{max} = 53.4 MPa; (**c**) t = 60 μs, P_{max} = 44 MPa; (**d**) t = 80 μs, P_{max} = 41 MPa; (**e**) t = 100 μs, P_{max} = 40 MPa; (**f**) t = 120 μs, P_{max} = 39 MPa, for the case presented in Figure 1.

https://doi.org/10.1017/S0263034608000426 Published online by Cambridge University Press

A larger spot at the beginning is imaged on a larger spot at the horizontal exit slit of the separator where the separation is done. But it is influenced only very little by the increase in the *y*-direction. The cut by this final corresponds to one band of nuclei on the 2D chart of nuclides. At the energy mentioned, it corresponds roughly to a line between isotopes of one element and an isobaric chain, as shown in Figure 1b. With larger spot size the width of this band is increased to not only one nuclide but up to four. In any case, even with the smallest spot size, it will not be possible to select only one single nuclide alone by the Super-FRS due to the nuclides in opposite direction.

To separate the remaining contaminants, the CR can be used as a radio frequency (RF)-mass filter. The process of stochastic cooling itself already causes a selection by the mass-to-charge ratio with a resolution of about 10^{-3} (Nolden *et al.*, 2000). An even better resolution could be achieved after the beam is cooled. However, ions of very similar mass to charge ratio can cause problems, these should be filtered out by the Super-FRS. This means the combination of Super-FRS and CR can provide good separation even for large beam spots, but the area of nuclides must not become so large that ions with very similar mass-to-charge ratio are transmitted. This condition defines a limit for the x-spot size at the target, but it does not define the size exactly. What exactly the next critical contaminant may be, also depends on the ratio of the two integers charge (q) and mass number (A). However, with a resolution of better than 10^{-3}, only ratios of $A/q = 2$ or $A/q = 2.5$ seem critical.

3. BEAM-TARGET PARAMETERS AND FURTHER DISCUSSION OF THE PROBLEM

In a fast extraction scheme, the projectile energy is practically deposited instantaneously (on a time scale of 50–100 ns) in the target that generates thermal pressure. The pressure gradient leads to hydrodynamic motion that generates deviatoric stresses in the material. If the level of these induced stresses is not low enough compared to the material yield strength, permanent damage is inflicted on to the target that in case of a brittle material like graphite, could result in target break up. Data on material properties of graphite provided by SGL (Private communication) shows that the tensile strength in range of our interest, significantly increases with temperature. It will therefore be advantageous to preheat the target by a defocused beam to a high temperature before the

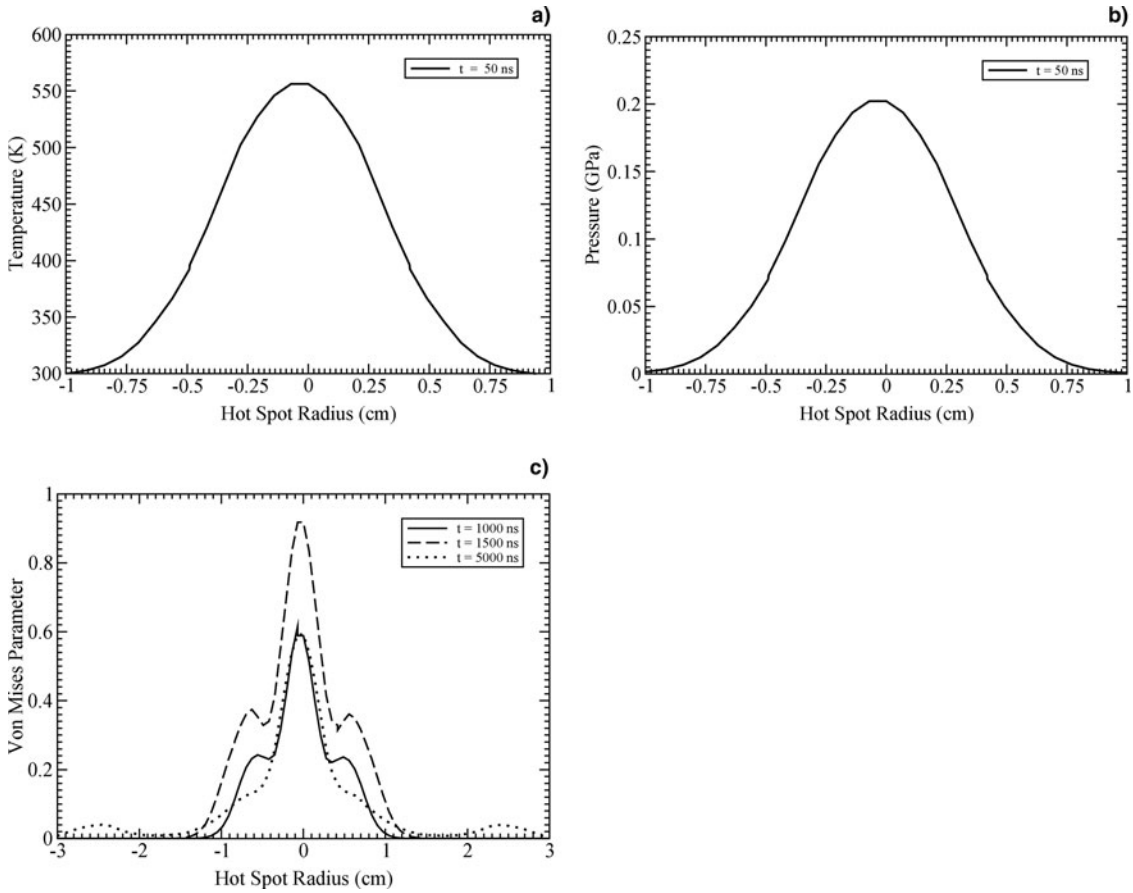

Fig. 5. $N = 6 \times 10^{10}$ uranium ions per bunch, particle energy = 1 GeV/u, $\tau = 50$ ns, circular focal spot with Gaussian transverse intensity distribution, $\sigma = 3$ mm, initial target temperature = 300 K, yield strength = 70 MPa: (**a**) temperature along spot radius at $t = 50$ ns; (**b**) pressure along spot radius at $t = 50$ ns; (**c**) Von Mises Parameter at three different times (maximum value at $t = 1500$ ns).

https://doi.org/10.1017/S0263034608000426 Published online by Cambridge University Press

actual experiments are performed. We therefore, have considered some cases in which an initial temperature of 2000 K has been assumed. In this section, we present the target and beam parameters that have been used in this study.

3.1. Target Initial Conditions

We consider a wheel shaped solid graphite target that has an inner radius, $R_1 = 13.5$ cm and an outer radius, $R_2 = 22.5$ cm. The target thickness is about 3 g/cm^2 (1.35 cm) that means the target mass is about 3 kg. The initial beam-target geometry is shown in Figure 2. The target is made of compressed powdered graphite with a density of 2.28 g/cm^3 and the SESAME equation-of-state data (Kerley, 2001) is used in the calculations.

In Super-FRS experiments, the target will be rotated and the beam will irradiate the target along a circle with radius = 18 cm. However, in the present work, we are mainly interested to study the development, propagation, and damping of the deviatoric stress waves generated in a single experiment in this particular target geometry. Data on material properties of graphite provided by SGL (2006) shows that the tensile strength in range of our interest, significantly increases with temperature. It will therefore be advantageous to preheat the target by a defocused beam to a high temperature before the actual experiments are performed. We therefore, have considered some cases in which an initial temperature of 2000 K has been assumed.

3.2. Beam Parameters

The beam comprises of uranium ions with a particle energy of 1 GeV/u that are delivered in a single bunch with a duration of 50 ns and the transverse intensity distribution in the focal spot is assumed to be Gaussian. We have optimized particle intensities that could be used for different focal spot sizes of practical importance from the point of view of isotope resolution and secondary beam transmission, as discussed in Sec. 2.

3.2.1. Beam Parameters for an Initially Cold Target

In the following, we present beam parameters for the cases in which the target is initially assumed to be at room temperature but the region that is irradiated by the beam (focal spot area) in a single experiment is heated to a temperature of about 600 K. Under these conditions, the tensile strength of graphite is on the order of 70 MPa (SGL, Private communication).

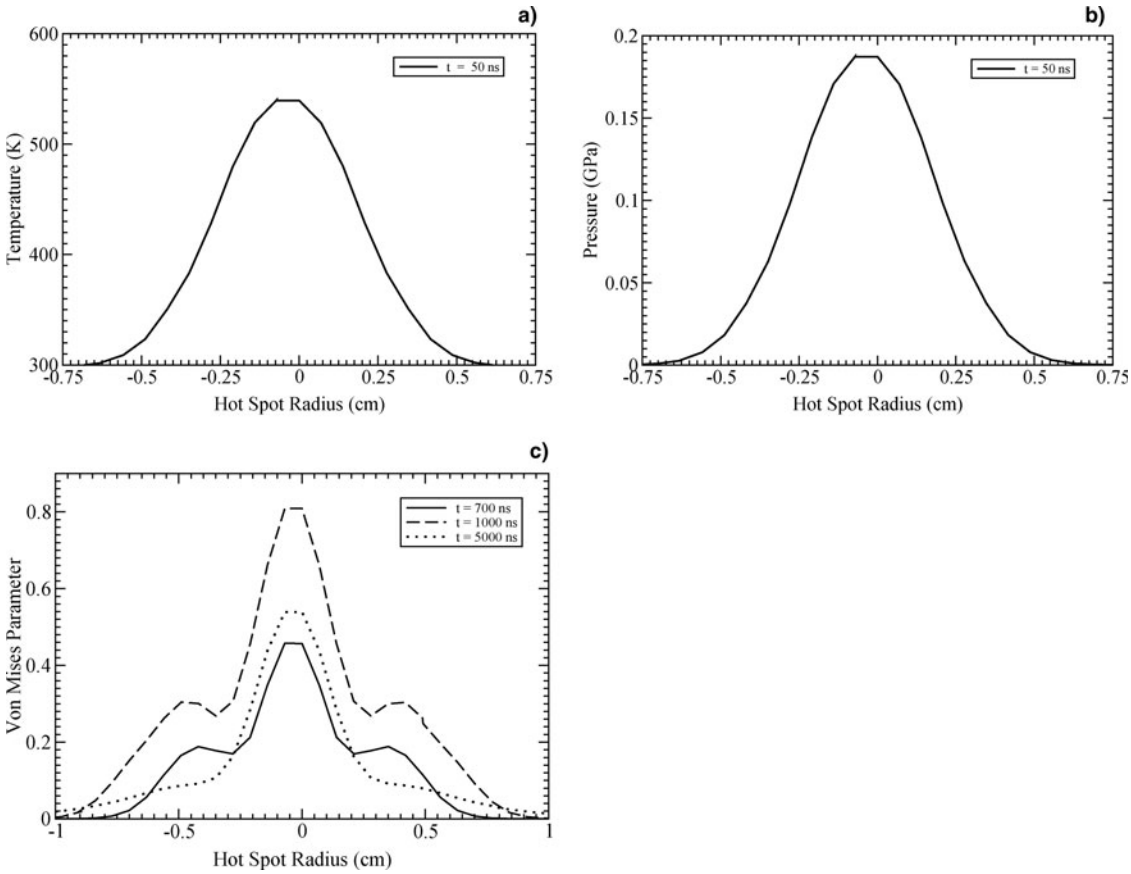

Fig. 6. $N = 2 \times 10^{10}$ uranium ions per bunch, particle energy = 1 GeV/u, $\tau = 50$ ns, circular focal spot with Gaussian transverse intensity distribution, $\sigma = 2$ mm, initial target temperature = 300 K, yield strength = 70 MPa : (**a**) temperature along spot radius at $t = 50$ ns; (**b**) pressure along spot radius at $t = 50$ ns; (**c**) Von Mises Parameter at three different times (maximum value at $t = 1000$ ns).

https://doi.org/10.1017/S0263034608000426 Published online by Cambridge University Press

Case I: circular focal spot with $\sigma = 4$ mm. In view of the discussion presented in Section 2, this is the upper limit on the focal spot size in x-direction for acceptable isotope resolution.
Case II: circular focal spot with $\sigma = 3$ mm.
Case III: circular focal spot with $\sigma = 2$ mm.

3.2.2. Beam Parameters for an Initially Heated Target

According to the data of material properties of graphite provided in SGL (Private communication), the yield strength of graphite in the temperature range of 1800–2000 K is about 100 MPa. Therefore, if the target is heated to within this range of temperature before performing fast extraction experiments, the target will tolerate a higher beam intensity. To heat the target to a temperature of 2000 K, one needs a specific energy deposition of about 2.95 kJ/g that means 9.1 MJ energy is needed to uniformly heat the entire target to 2000 K. Total energy in the beam with full uranium intensity of 5×10^{11} ions per bunch, is 19 kJ. About 25% beam energy is absorbed in the target that implies that in every experimental shot, about 4.75 kJ energy is deposited in the production target. This requires that the target should be preradiated at least 2200 times by a defocused beam to achieve uniform heating to this temperature. With a repetition rate of 1 Hz, this means the target should be heated for about 40 s. It is however, to be noted that during the heating process, a fraction of the deposited power will be lost due to radiation emission and in practice, one would require a higher number of preheat shots. A self consistent detailed study of this problem is intended for future works.

In the present study, assuming that the target is preheated to 2000 K, we have carried out simulations using different focal spot parameters given below. The main purpose of this study is to determine a configuration that can be used for the highest intensity of the uranium beam, namely, 5×10^{11} ions per bunch.
Case IV: circular focal spot with $\sigma = 4$ mm.
Case V: elliptic focal spot with $\sigma_X = 4$ mm and $\sigma_Y = 6$ mm.
Case VI: elliptic focal spot with $\sigma_X = 4$ mm and $\sigma_Y = 8$ mm.
Case VII: elliptic focal spot with $\sigma_X = 4$ mm and $\sigma_Y = 11$ mm.

It is to be noted that recommended operating target temperature (Heidenreich, 2002) taking into account a tolerable sublimation rate of about 10 mg g^{-1} $year^{-1}$, is about 1800 K. One can therefore consider an initial target

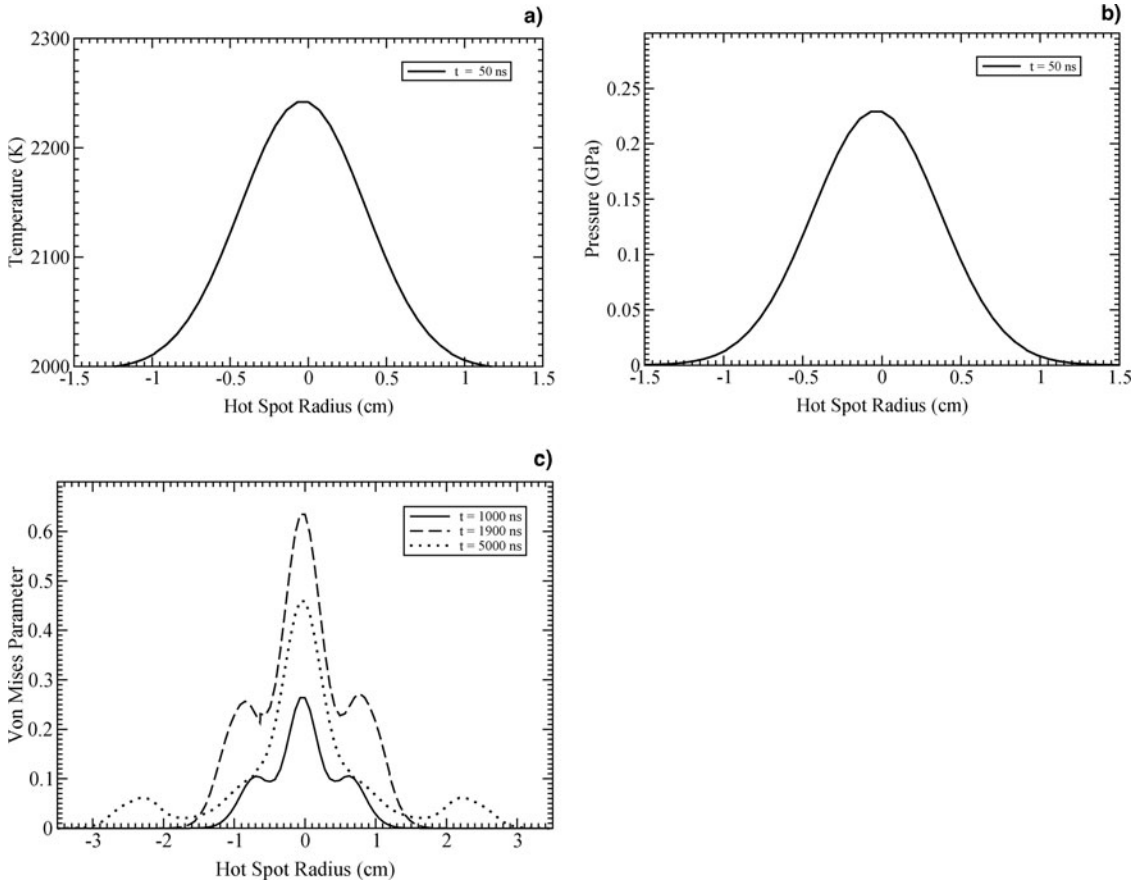

Fig. 7. $N = 2 \times 10^{11}$ uranium ions per bunch, particle energy = 1 GeV/u, $\tau = 50$ ns, circular focal spot with Gaussian transverse intensity distribution, $\sigma = 4$ mm, initial target temperature = 2000 K, yield strength = 100 MPa: (**a**) temperature along spot radius at $t = 50$ ns; (**b**) pressure along spot radius at $t = 50$ ns; (**c**) Von Mises Parameter at three different times (maximum value at $t = 1900$ ns).

https://doi.org/10.1017/S0263034608000426 Published online by Cambridge University Press

temperature of 1800 K without suffering much reduction in the yield strength.

4. NUMERICAL SIMULATION RESULTS

In this section, we present simulation results of different cases noted in Section 3 that have been obtained using a 2D hydrodynamic computer code, BIG2 (Fortov *et al.*, 1996). This is based on a Godunov type scheme and it includes energy deposition by projectile ions while equation of state data is either used from a semi-empirical model (Bushman *et al.*, 1993; Lomonosov, 2007; Lomonosov & Tahir, 2008) or from the SESAME data bank (Kerley, 2001). Since the range of 1 GeV/u uranium particles is longer than the thickness of the target, energy deposition is fairly uniform along the particle trajectory. This means that the problem initially is 2D and therefore use of the BIG2 code is valid for all the cases reported in this paper. We note that on longer time scale, the surface temperature will reduce due to radiation losses and a temperature gradient will be generated in longitudinal direction. This will lead to a pressure gradient, however this will be less steeper than the gradient in the radial direction. Therefore, if the target survives the deviatoric stresses generated by the pressure gradient in radial direction, it will also survive those generated in longitudinal direction.

4.1. Simulation Results Using an Initially Cold Target

In the following, we present simulation results of different cases described in Section 3.2.1 that assume an initial target temperature of 300 K (room temperature).

Case I: circular focal spot with $\sigma = 4$ mm. The beam-target geometry at $t = 50$ ns (when the beam has just delivered its energy) is shown in Figure 2. Beam is vertically incident onto the target and the temperature as well as the pressure increases in the beam heated region. The focal spot has a circular shape with $\sigma = 4$ mm and simulations have shown that the target can tolerate a maximum beam intensity of up to 10^{11} ions per spill.

In Figures 3a and 3b, we plot the temperature and pressure along radius of the hot spot, respectively. Gaussian nature of the beam intensity in transverse direction is reflected in these figures. It is seen that a maximum temperature of about

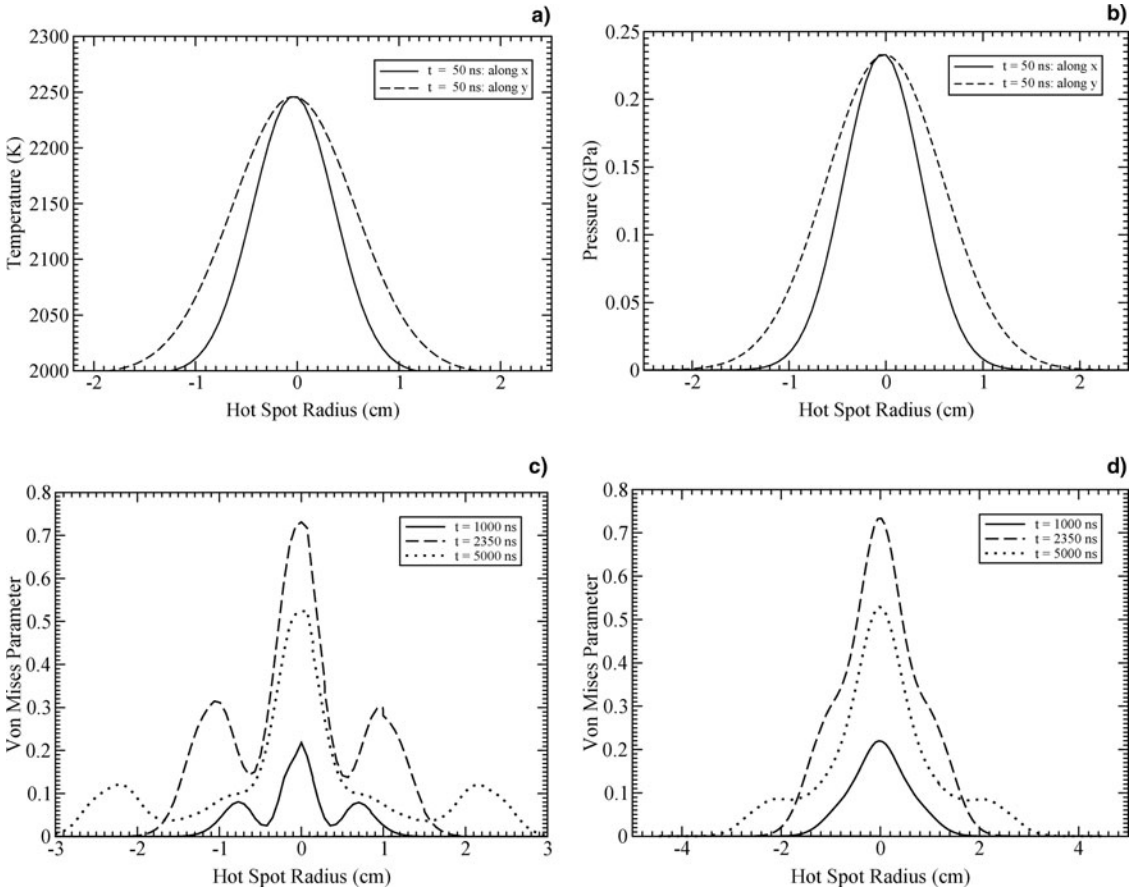

Fig. 8. $N = 3 \times 10^{11}$ uranium ions per bunch, particle energy = 1 GeV/u, $\tau = 50$ ns, elliptic focal spot with Gaussian transverse intensity distribution, $\sigma_X = 4$ mm, $\sigma_Y = 6$ mm, initial target temperature = 2000 K, yield strength = 100 MPa: (**a**) temperature along spot radius at $t = 50$ ns; (**b**) pressure along spot radius at $t = 50$ ns; (**c**) Von Mises Parameter in the x-direction; (**d**) Von Mises Parameter in the y-direction at three different times (maximum value at $t = 2350$ ns).

https://doi.org/10.1017/S0263034608000426 Published online by Cambridge University Press

550 K and a maximum pressure on the order of 200 MPa is produced at the center of the Gaussian. The pressure gradient generates hydrodynamic motion that leads to shear and deviatoric stress in the material. The material retains its original properties if it remains in elastic regime despite these stresses that requires that the Von Mises parameter, M is less than 1. In Figure 3c, is plotted the Von Mises parameter along the radius of the hot zone at three different times. It is seen that a maximum value of M of about 0.8 is achieved at $t = 2$ μs that decreases to about 0.5 at 5 μs due to spreading out of the pressure and stress waves from the central hot region. This is seen in Figures 4a–4f where we plot pressure isolines in the target at different times.

Figure 4a shows that at $t = 5$ μs, the maximum pressure has been reduced to about 55 MPa from an initial value of about 200 MPa and the focal spot area has become significantly larger compared to that in Figure 2 at $t = 50$ ns. Figure 4b is plotted at $t = 15$ μs that shows the reflection of the pressure wave from the target boundary along y-direction and spreading out of pressure in x-direction. The maximum pressure at the center of the hot spot is now on the order of 53 MPa. Subsequent figures show time evolution of pressure along the target and multiple reflection of the pressure waves from the boundary. Figure 5f shows that at $t = 120$ μs, the pressure waves have propagated through the entire target and the maximum pressure has been substantially reduced in the beam heated region. A similar behavior has been observed for the deviatoric stress waves. One can therefore conclude that within 1 s, before the target is irradiated the second time, the deviatoric stress induced by the previous experimental shot will be damped out and the target material would retain its original state.

Case II: circular focal spot with $\sigma = 3$ mm. Simulations have shown that one can use a maximum beam intensity of up to 6×10^{10} ions per spill in this case. The temperature and the pressure profiles at $t = 50$ ns are plotted in Figures 5a and 5b, respectively. It is seen that the maximum temperature is 550 K whereas the maximum pressure is about 200 MPa. The Von Mises parameter, M, along the radius of the hot zone at three different times is shown in Figure 5c. It is seen that at $t = 1.5$ μs, a maximum value of M on the order of 0.9 is achieved that reduces to 0.6 at $t = 5$ μs that indicates that the target will survive in this experiment.

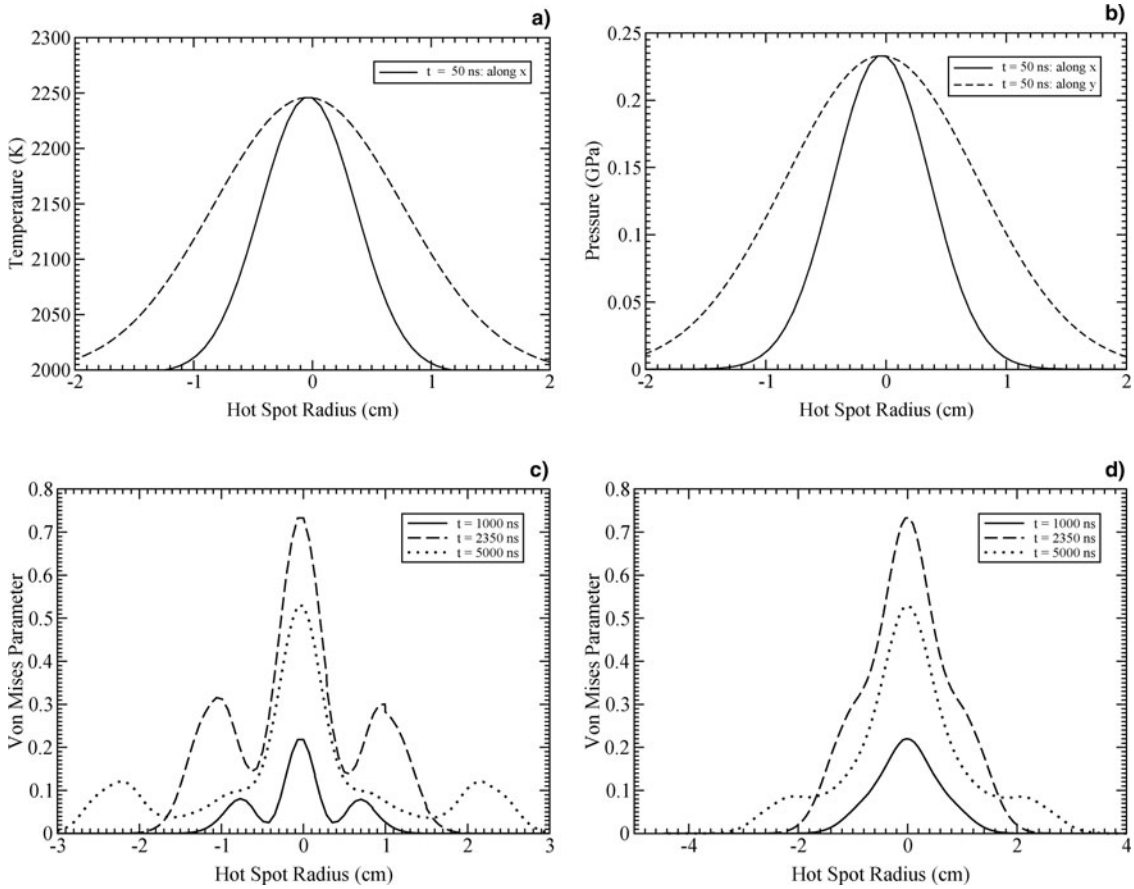

Fig. 9. $N = 4 \times 10^{11}$ uranium ions per bunch, particle energy = 1 GeV/u, $\tau = 50$ ns, elliptic focal spot with Gaussian transverse intensity distribution, $\sigma_X = 4$ mm, $\sigma_Y = 8$ mm, initial target temperature = 2000 K, yield strength = 100 MPa: (**a**) temperature along spot radius at $t = 50$ ns; (**b**) pressure along spot radius at $t = 50$ ns; (**c**) Von Mises Parameter in the x-direction; (**d**) Von Mises Parameter in the y-direction at three different times (maximum value at $t = 2350$ ns).

https://doi.org/10.1017/S0263034608000426 Published online by Cambridge University Press

Case III: circular focal spot with σ = 2 mm. According to our simulations, with this spot size, the target can tolerate up to 2×10^{10} ions per spill. Temperature and pressure profiles at $t = 50$ ns are shown in Figures 6a and 6b, respectively while the Von Mises parameter at three different times is plotted in Figure 6c. This parameter achieves a maximum value of 0.8 at $t = 1$ μs that shows that the target will survive in this experiment.

4.2. Simulation Results Using a Preheated Target

In the following cases, the production target is heated to an initial temperature of 2000 K and the yield strength is considered to be 100 MPa.

Case IV: circular focal spot with σ = 4 mm. Simulations have shown that the target can tolerate a beam intensity of up to 2×10^{11} ions per spill with this focal spot size. This is seen from Figure 7c which shows the Von Mises parameter in the beam heated region at three different times with a maximum value of about 0.6 at $t = 1.9$ μs. The temperature and pressure profiles at $t = 50$ ns are plotted in Figures 7a and 7b, respectively.

Since according to analysis presented in Section 2, the maximum value of σ along the x-direction should not exceed 4 mm, one needs to consider an elliptic focal spot with larger values of σ_Y to increase the focal spot area as given below.

Case V: elliptic focal spot with σ_X = 4 mm and σ_Y = 6 mm. The focal spot area is 50% larger than in case IV. Since the ellipticity is not very large, the deviatoric stress generated in the target is close to that produced by a circular spot. Therefore one can use a higher beam intensity in the same proportion as increase in the beam spot area in the two cases. Simulations have confirmed that the target will tolerate 3×10^{11} ions per spill for these conditions.

Figures 8a and 8b show temperature and pressure profiles along the x and y directions at $t = 50$ ns. It is seen that the temperature increases from the initial value of 2000 K to 2250 K at the center of the hot zone while the corresponding maximum pressure is 225 MPa. It is to be noted that when the target is preheated to 2000 K, the material expands until a low equilibrium pressure is achieved. From the equation of state model one finds that the density corresponding to these equilibrium conditions is 2.167 g/cm^3 compared to 2.28 g/cm^3 at room temperature.

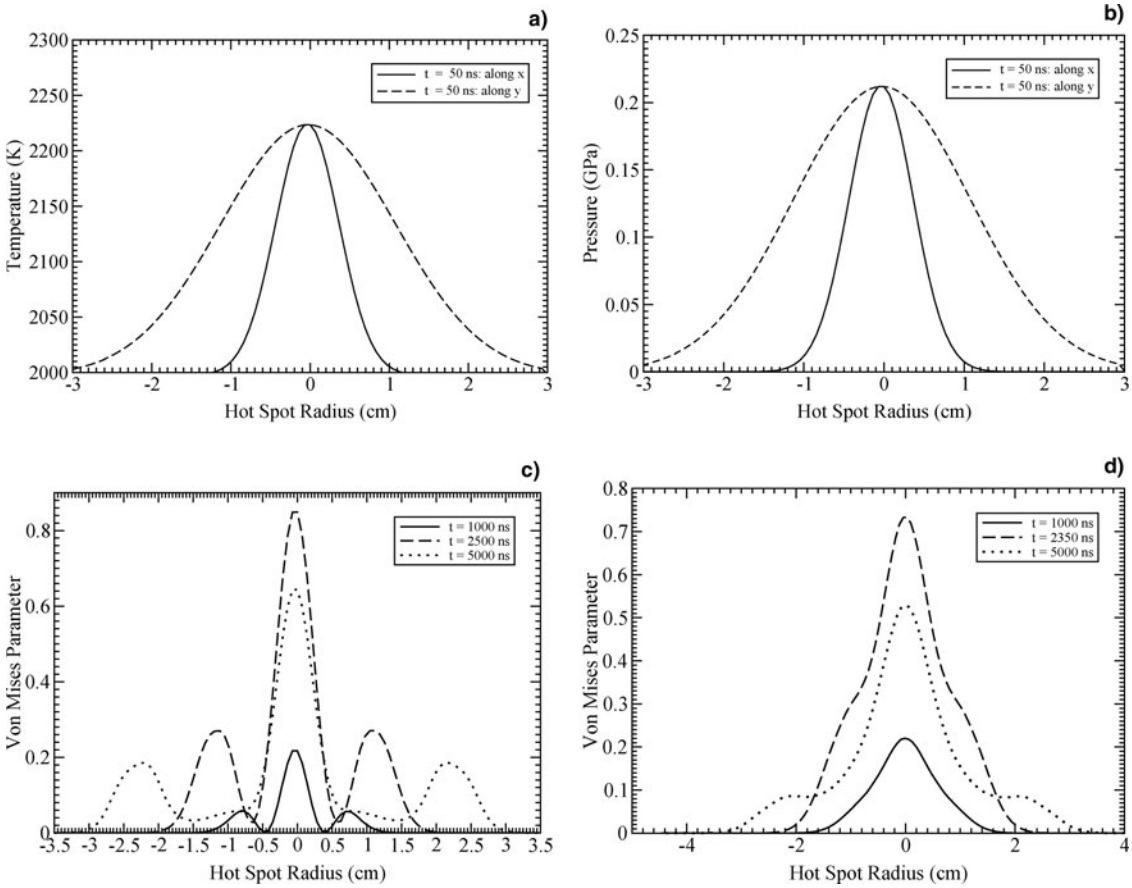

Fig. 10. $N = 5 \times 10^{11}$ uranium ions per bunch, particle energy = 1 GeV/u, $\tau = 50$ ns, elliptic focal spot with Gaussian transverse intensity distribution, $\sigma_X = 4$ mm, $\sigma_Y = 11$ mm, initial target temperature = 2000 K, yield strength = 100 MPa: (**a**) temperature along spot radius at $t = 50$ ns; (**b**) pressure along spot radius at $t = 50$ ns; (**c**) Von Mises Parameter in the x-direction; (**d**) Von Mises Parameter in the y-direction at three different times (maximum value at $t = 2500$ ns).

https://doi.org/10.1017/S0263034608000426 Published online by Cambridge University Press

Figure 8c shows the Von Mises parameter in hot zone at three different times along the *x*-direction. It is seen that a maximum value of about 0.7 is achieved at $t = 2.35$ μs that decreases to 0.5 at $t = 5$ μs. It is interesting to note that due to steeper pressure gradient in the *x*-direction, the effect of stronger hydrodynamic motion spreading outwards is seen in all three curves (formation of two smaller peaks on both sides of the main peak is to be noted).

Figure 8d presents plots of the Von Mises parameter at the same three time points as Figure 8c, but along the *y*-direction. It is seen that due to the weaker pressure gradient in this direction, the spread of the deviatoric stress waves is slower, and the typical two peak structure starts to develop at $t = 5$ μs.

Case VI: elliptic focal spot with $\sigma_X = 4$ mm and $\sigma_Y = 8$ mm. Simulations have shown that one can use up to $N = 4 \times 10^{11}$ ions per spill with these beam parameters. Temperature and pressure profiles along the *x* and *y*-direction at $t = 50$ ns are plotted in Figures 9a and 9b, respectively. Profiles of the Von Mises parameter along the *x* and *y*-direction at three different times are given in Figures 9c and 9d, respectively. These profiles show a behavior similar to the corresponding profiles in case V.

Case VII: elliptic focal spot with $\sigma_X = 4$ mm and $\sigma_Y = 11$ mm. This case has been designed for the highest uranium beam intensity of 5×10^{11}. Simulations have shown that one must use a large focal spot area with $\sigma_X = 4$ mm and $\sigma_Y = 11$ mm. Due to larger ellipticity of the focal spot geometry, the linear relationship between the focal spot area and the beam intensity does not work. Temperature and pressure profiles in the hot zone along the *x* and *y*-direction are plotted in Figures 10a and 10b, respectively while the profiles of Von Mises parameter at three different times along the *x* and *y*-direction are plotted in Figures 10c and 10d, respectively. Elliptic nature of the spatial beam intensity profile is reflected in these profiles.

5. CONCLUSIONS

Two-dimensional numerical simulations have been carried out to design a viable solid graphite target for the Super-FRS fast extraction scheme that can be used over an extended period of time. Maximum values of beam intensity, N, that the target will tolerate for different sizes of the focal spot that are fixed by considerations of good isotope resolution and acceptable level of secondary beam transmission, have been determined. It has been found that one can use $N = 2 \times 10^{10}$, 6×10^{10}, and 10^{11} for focal spot sizes with $\sigma = 2$, 3, and 4 mm, respectively. In these calculations, the target initially is assumed to be at room temperature whereas the region irradiated by the focal spot is heated to about 600 K by the beam and correspondingly a yield strength of 70 MPa is considered in these simulations.

Since the yield strength increases to about 100 MPa in the temperature range of 1800–2000 K, simulations have also been carried out assuming a target preheated to a temperature of 2000 K. These simulations have shown that one may use a beam intensity of 2×10^{11} for a focal spot with $\sigma = 4$ mm. However for higher intensities, one needs to use an elliptic focal spot which has $\sigma_X = 4$ mm and a larger value of σ_Y. It has been found that one may can use beam intensities of 3×10^{11}, 4×10^{11}, and 5×10^{11} uranium ions per spill for $\sigma_Y = 6$, 8, and 11 mm, respectively.

ACKNOWLEDGMENTS

The authors would like to thank H. Geissel, A. Kelic, K. Sümmerer, M. Winkler for many useful discussions and G. Kerley for providing the EOS data for graphite. This work was financially supported by the BMBF, Germany and RFBR grant No. 06-02-04011-NNIOa, Russia.

REFERENCES

Bushman, A.V., Kanel, G.I., Ni, A.L. & Fortov, V.E. (1993). Thermophysics and dynamics of intense pulsed loadings. *London: Taylor and Francis*.

Dolinskii, A., Beller, P., Beckert, K., Franzke, B., Nolden, F. & Steck, M. (2004). Optimized lattice for the collector ring (CR). *Nucl. Instrum. Methods A* **532**, 483.

Fortov, V.E., Goel, B., Munz, C.-D., Ni, A.L., Shutov, A. & Vorobiev, O.Yu. (1996). Numerical simulations of non-stationary fronts and interfaces by the Godunov method in moving grids. *Nucl. Sci. Eng*. **123**, 169.

Geissel, H., Weick, H., Münzenberg, G., Chichkine, V., Yavor, M., Aumann, T., Behr, K.H., Böhmer, A., Brünle, A., Burkahrd, K., Benlliure, J., Cortina-Gil, D., Chulkov, L., Dael, A., Ducret, J.-E., Emling, H., Franczak, B., Friese, J., Gastineau, B., Gerl, J., Gernhäuser, R., Hellström, M., Johnson, B., Kojouharova, J., Kulessa, R., Kindler, B., Kurz, N., Lommel, B., Mittig, W., Moritz, G., Mühle, Nolen, J.A., Nyman, G., Rousell-Chomaz, P., Scheindenberger, C., Schmidt, K.-H., Schrieder, G., Sherrill, B.M., Simon, H., Sümmerer, K., Tahir, N.A., Vysotsky, V., Wollnik, H. & Zeller, A.F. (2003). The Super-FRS project at GSI. *Nucl. Instrum. Methods Phys. Res. B* **204**, 71.

Heidenreich, G. (2002). Carbon and beryllium targets at PSI. *AIP Conf. Proc. 642: High Intensity and High Brightness Hadron Beams* **642**, 124.

Henning, W.F. (2004). The future GSI facility. *Nucl. Instrum. Methods Phys. Res. B* **214**, 155.

Hoffmann, D.H.H., Blazevic, A., Ni, P., Rosmej, O., Roth, M., Tahir, N.A., Tauschwitz, A., Udrea, S., Varentsov, D., Weyrich, K. & Maron, Y. (2005). Present and future perspectives of high energy density physics with intense ions and laser beams. *Laser Part. Beams* **23**, 47.

Iwasa, N., Geissel, H., Muenzenberg, G., Scheindenberger, C., Schwab, Th. & Wolnik, H. (1997). MOCADI, a universal Monte Carlo code for the transport of heavy ions through matter with ion optical systems. *Nucl. Instrum. Methods Phys. Res. B* **126**, 284.

Kerley, G.I. (2001). Multi-component multiphase equation-of-state for carbon. *Sandia Nat. Lab. Rep*. **SAND2001–2619**.

Lomonosov, I.V. (2007). A multi-phase equation-of-state for aluminum. *Laser Part. Beams* **25**, 567.

Lomonosov, I.V. & Tahir, N.A. (2008). Theoretical investigation of shock wave instability in metals. *Appl. Phys. Lett*. **92**, 101905.

Lopez Cela, J.J., Piriz, A.R., Serena Moreno, M. & Tahir, N.A. (2006). Numerical simulations of Rayleigh-Taylor instability in elastic solids. *Laser Part. Beams* **24**, 427.

Nolden, F., Beckert, F., Caspers, F., Franzke, B., Menges, R., Schwinn, A. & Steck, M. (2000). Stochastic cooling in the ESR. *Nucl. Instrum. Methods Phys. Res. A* **441**, 219.

Piriz, A.R., Portugues, R.F., Tahir, N.A. & Hofmann, D.H.H. (2002). Implosion of multilayered cylindrical targets driven by intense heavy ion beams. *Phys. Rev. E* **66**, 056403.

Piriz, A.R., Tahir, N.A., Hoffmann, D.H.H. & Temporal, M. (2003). Generation of a hollow ion beam: Calculation of the rotation frequency required to accomodate symmetry constraint. *Phys. Rev. E* **67**, 017501.

Piriz, A.R., Temporal, M., Lopez Cela, J.J., Tahir, N.A. & Hoffmann, D.H.H. (2005). Rayleigh-Taylor instability in elastic solids. *Phys. Rev. E* **72**, 056313.

Piriz, A.R., Lopez Cela, J.J., Serena Moreno, M., Tahir, N.A. & Hoffmann, D.H.H. (2006). Thin plate effects in the Rayleigh-Taylor instability of elastic solids. *Laser Part. Beams* **24**, 275.

Piriz, A.R., Tahir, N.A., Lopez Cela, J.J., Cortazar, O.D., Serna Moreno, M.C., Temporal, M. & Hoffmann, D.H.H. (2007). Analytic models for the design of the LAPLAS target. *Contrib. Plasma Phys*. **47**, 213.

Piriz, A.R., Lopez Cela, J.J., Serna Moreno, M.C., Cortazar, O.D., Tahir, N.A. & Hoffmann, D.H.H. (2007). A new approach to Rayleigh-Taylor instability: Applications to accelerated elastic solids. *Nucl. Instrum. Methods Phys. Res. A* **577**, 250.

Tahir, N.A., Hoffmann, D.H.H., Spiller, P. & Bock, R. (1999). Heavy-ion-induced hydrodynamic effects in solid targets. *Phys. Rev. E* **60**, 4715.

Tahir, N.A., Hoffmann, D.H.H., Kozyreva, A., Shutov, A., Maruhn, J.A., Neuner, U., Tauschwitz, A., Spiller, P. & Bock, R. (2000*a*). Shock compression of condensed matter using intense beams of energetic heavy ions. *Phys. Rev. E* **61**, 1975.

Tahir, N.A., Hoffmann, D.H.H., Kozyreva, A., Shutov, A., Maruhn, J.A., Neuner, U., Tauschwitz, A., Spiller, P. & Bock, R. (2000*b*). Equation-of-state properties of high-energy-density matter using intense heavy ion beams with an annular focal spot. *Phys. Rev. E* **62**, 1224.

Tahir, N.A., Kozyreva, Spiller, P., Hoffmann, D.H.H. & Shutov, A. (2001*a*). Necessity of bunch compression for heavy-ion-induced hydrodynamics and studies of beam fragmentation in solid targets at a proposed synchrotron facility. *Phys. Rev. E* **63**, 036407.

Tahir, N.A., Hoffmann, D.H.H., Kozyreva, A., Tauschwitz, A., Shutov, A., Maruhn, J.A., Spiller, P., Nuener, U., Jacoby, J., Roth, M., Bock, R., Juranek, H. & Redmer, R. (2001*b*). Metallization of hydrogen using heavy-ion-beam implosion of multi-layered targets. *Phys. Rev. E* **63**, 016402.

Tahir, N.A., Juranek, H., Shutov, A., Redmer, R., Piriz, A.R., Temporal, M., Varentsov, D., Udrea, S., Hoffmann, D.H.H., Deutsch, C., Lomonosov, I. & Fortov, V.E. (2003*a*). Influence of the equation of state on the compression and heating of hydrogen. *Phys. Rev. B* **67**, 184101.

Tahir, N.A., Winkler, M., Kojouharova, J., Rousell-Chomaz, P., Chichkine, V., Geissel, H., Hoffmann, D.H.H., Kindler, B., Landre-Pellemoine, F., Lommel, B., Mittig, W., Münzenberg, G., Shutov, A., Weick, H. & Yavor, M. (2003*b*). High-power production targets for the Super-FRS using a fast extraction scheme. *Nucl. Instrum. Methods Phys. Res. B* **204**, 282.

Tahir, N.A., Adonin, A., Deutsch, C., Fortov, V.E., Grandjouan, N., Geil, B., Gryaznov, V., Hoffmann, D.H.H., Kulish, M., Lomonosov, I.V., Mintsev, V., Ni, P., Nikolaev, D., Piriz, A.R., Shilkin, N., Spiller, P., Shutov, A., Temporal, M., Ternovoi, V., Udrea, S. & Varentsov, D. (2005*a*). Studies of heavy ion-induced high-energy density states in matter at the GSI Darmstadt SIS-18 and future FAIR facility. *Nucl. Instrum. Methods Phys. Res. A* **544**, 16.

Tahir, N.A., Deutsch, C., Fortov, V.E., Gryaznov, V., Hoffmann, D.H.H., Kulish, M., Lomonosov, I.V., Mintsev, V., Ni, P., Nikolaev, D., Piriz, A.R., Shilkin, N., Spiller, P., Shutov, A., Temporal, M., Ternovoi, V., Udrea, S. & Varentsov, D. (2005*b*). Proposal for the study of thermophysical properties of high-energy-density matter using current and future heavy ion accelerator facilities at GSI Darmstadt. *Phys. Rev. Lett*. **95**, 035001.

Tahir, N.A., Weick, H., Iwase, H., Geissel, H., Hoffmann, D.H.H., Kindler, B., Lommel, B., Radon, T., Münzenberg, G. & Sümmerer, K. (2005*c*). Calculations of high-power production target and beamdump for the GSI future Super-FRS for a fast extraction scheme at the FAIR facility. *J. Phys. D: Appl. Phys*. **38**, 1828.

Tahir, N.A., Goddard, B., Kain, V., Schmidt, R., Shutov, A., Lomonosov, I.V., Piriz, A.R., Temporal, M., Hoffmann, D.H.H. & Fortov, V.E. (2005*d*). Impact of 7-Tev/c large Hadron collider proton beam on a copper target. *J. Appl. Phys*. **97**, 083532.

Tahir, N.A., Kain, V., Schmidt, R., Shutov, A., Lomonosov, I.V., Gryaznov, V., Piriz, A.R., Temporal, M., Hoffmann, D.H.H. & Fortov, V.E. (2005*e*). The CERN large Hadron collider as a tool to study high-energy-density physics. *Phys. Rev. Lett*. **94**, 135004.

Tahir, N.A., Spiller, P., Udrea, S., Cortazar, O.D., Deutsch, C., Fortov, V.E., Gryaznov, V., Hoffmann, D.H.H., Lomonosov, I.V., Ni, P., Piriz, A.R., Shutov, A., Temporal, M. & Varentsov, D. (2006). Studies of equation-of-state properties of high-energy density matter using intense heavy ion beams at the future FAIR facility: The HEDgeHOB collaboration. *Nucl. Instrum. Methods Phys. Res. B* **245**, 85.

Tahir, N.A., Spiller, P., Shutov, A., Lomonosov, I.V., Gryaznov, V., Piriz, A.R., Wouchuk, G., Deutsch, C., Fortov, V.E., Hoffmann, D.H.H. & Schmidt, R. (2007*a*). HEDgeHOB: High-energy-density matter generated by heavy ion beams at the future facility for antiprotons and ion research. *Nucl. Instrum. Methods Phys. Res. A* **577**, 238.

Tahir, N.A., Piriz, A.R., Shutov, A., Lomonosov, I.V., Gryaznov, V., Wouchuk, G., Deutsch, C., Spiller, P., Fortov, V.E., Hoffmann, D.H.H. & Schmidt, R. (2007*b*). Survey of theoretical work for the proposed HEDgeHOB collaboration: HIHEX and LAPLAS. *Contrib. Plasma Phys*. **47**, 223.

Tahir, N.A., Schmict, R., Brugger, M., Lomonosov, I.V., Shutov, A., Piriz, A.R., Udrea, S., Hoffmann, D.H.H. & Deutsch, C. (2007*c*). Prospects of high energy density research using the CERN Super Proton Synchrotron. *Laser Part. Beams*. **25**, 639.

Tahir, N.A., Kim, V., Matveichev, A., Ostrik, A., Lomonosov, I.V., Piriz, A.R., Weick, Lopez Cela, J.J. & Hoffmann, D.H.H. (2007*d*). Numerical modeling of heavy ion induced thermal stress waves in solid targets. *Laser Part. Beams* **25**, 523.

Tahir, N.A., Kim, V., Grigoriev, D.A., Piriz, A.R., Weick, H., Geissel, H. & Hoffmann, D.H.H. (2007*e*). High energy

density physics problems related to liquid jet lithium target for Super-FRS fast extraction scheme. *Laser Part. Beams* **25**, 295.

Tahir, N.A., Kim, V.V., Matveichev, A.V., Ostrik, A.V., Shutov, A.V., Lomonosov, I.V., Piriz, A.R., Lopez Cela, J.J. & Hoffmann, D.H.H. (2008). High energy density and beam induced stress related issues in solid graphite Super-FRS fast extraction targets. *Laser Part. Beams*. **26**, 273.

Temporal, M.J.J., Piriz, A.R., Grandjouan, N., Tahir, N.A. & Hoffmann, D.H.H. (2003). Numerical analysis of a multilayered cylindrical target compression driven by a rotating intense heavy ion beam. *Laser Part. Beams* **21**, 609.

Temporal, M., Lopez-Cela, J.J., Piriz, A.R., Grandjouan, N., Tahir, N.A. & Hoffmann, D.H.H. (2005). Compression of a cylindrical hydrogen sample driven by an intense co-axial heavy ion beam. *Laser Part. Beams*. **23**, 137.

https://doi.org/10.1017/S0263034608000426 Published online by Cambridge University Press